Production d'énergie (hydraulique, thermique et nucléaire)

STRATIFICATION THERMIQUE. UN POINT DE VUE INDUSTRIEL

THERMAL STRATIFICATIONS. AN INDUSTRIAL POINT OF VIEW

96NB00095

Direction des Etudes et Recherches

EDF
Electricité de France

Direction des Etudes et Recherches

SERVICE APPLICATIONS DE L'ELECTRICITE ET ENVIRONNEMENT
Département Laboratoire National d'Hydraulique

Novembre 1995

PENIGUEL C.

STRATIFICATION THERMIQUE. UN POINT DE VUE INDUSTRIEL

THERMAL STRATIFICATIONS. AN INDUSTRIAL POINT OF VIEW

Pages : 19

96NB00095

Diffusion : J.-M. Lecœuvre
EDF-DER
Service IPN. Département SID
1, avenue du Général-de-Gaulle
92141 Clamart Cedex

ISSN 1161-0611

SYNTHÈSE :

Dans les REP, des endommagements (fissures) ont été détectés sur les faces internes des tuyauteries d'arrivée d'eau du générateur de vapeur lors de l'apparition d'une stratification thermique.

Cette note expose certaines études des écoulements en condition de fonctionnement, conduisant l'apparition d'écoulements stratifiés stables. Deux géométries, correspondant à différentes maquettes étudiées à EDF et au CEA ont été examinées. Des simulations numériques ont été effectuées à l'aide du code ESTET. On observe une bonne corrélation au niveau de la température moyenne, mais il semble que la modélisation actuelle de la variance de température ne reproduise pas correctement les phénomènes fluctuants. Il apparaît que pour un écoulement stratifié stable, il faille tenir compte de la conduction de paroi.

Ceci nous a conduit à élaborer un nouvel outil numérique (SYRTHES) pour calculer le champ thermique à l'intérieur de la paroi, et le couplage thermique entre le fluide et le solide à l'interface.

On présente brièvement certains exemples industriels illustrant l'emploi de cet outil numérique.

EXECUTIVE SUMMARY :

In PWR's, mechanical damages (cracks) have been detected at the internal faces of steam generator feedwater piping when thermal stratification occurs.

This paper reports some studies of flows under operating conditions leading to of a stable stratified flow. Two geometries corresponding to different mock-up studied at EDF and CEA have been investigated. Numerical simulations have been performed with the code ESTET. Good agreement is observed on the mean temperature but it seems that the present modelling of the temperature variance fails to reproduce correctly the fluctuating phenomena. It appears that with a stably stratified flow, wall conduction should be taken into account.

It lead us to create a new numerical tool (SYRTHES) to compute the thermal field inside the wall, and the thermal coupling between the fluid and the solid at the interface.

Some industrial examples illustrating the use of such a numerical tool are briefly presented.

Thermal stratification
An industrial point of view

C. Péniguel
EDF/LNH, 6 quai Watier BP 49 F-78401 Chatou

INTRODUCTION

Cracks have appeared in a number of pressurized water reactors (PWR's) at the internal faces of pipes. Among other factors, thermal stratification phenomena seem to be quite good candidates to partly explain these mechanical damages. This problem may affect for example, steam generator feed-water systems, pressurizer surgeline and safety injection piping sytems.

By definition, a flow is said to be stratified when it is possible to identify several rather thin horizontal layers at different temperatures. This situation may arise under certain operating conditions, and particularly in presence of reduced mass flow. In piping systems, due to gravity effect, hot water fills the top portion of the pipe section and the cold and therefore heavier water settles down at the bottom. This temperature distribution results in a mechanical loading characterized by a differential expansion, which may cause potential damage to the piping system.

Stratification phenomena have been observed in laboratory experiments, and studied numerically (see [1], [2], [3], [4]). These have also been detected on site, using non invasive techniques (see Prud'homme [5]).

To improve the knowledge on stratifications, several mock-up (Super Nimbus, Fluo, etc...) have been designed to study parameters likely to influence the stratification. The main objectives being to gain some understanding on the stratification phenomenon, and use the experimental data to validate computer modelling, rather than provide a realistic representation of an existing piping system, with appropriate flow conditions.

Another aspect looked at was the temperature fluctuations, which may be responsible for thermal striping.

1. PRESENTATION OF THE EXPERIMENTAL FACILITIES

Super Nimbus

As stated in the introduction, the mock has been designed to help understanding phenomena governing the formation of stable stratified states. For this reason it has been made of perspex which allows visualisation (figure 1).

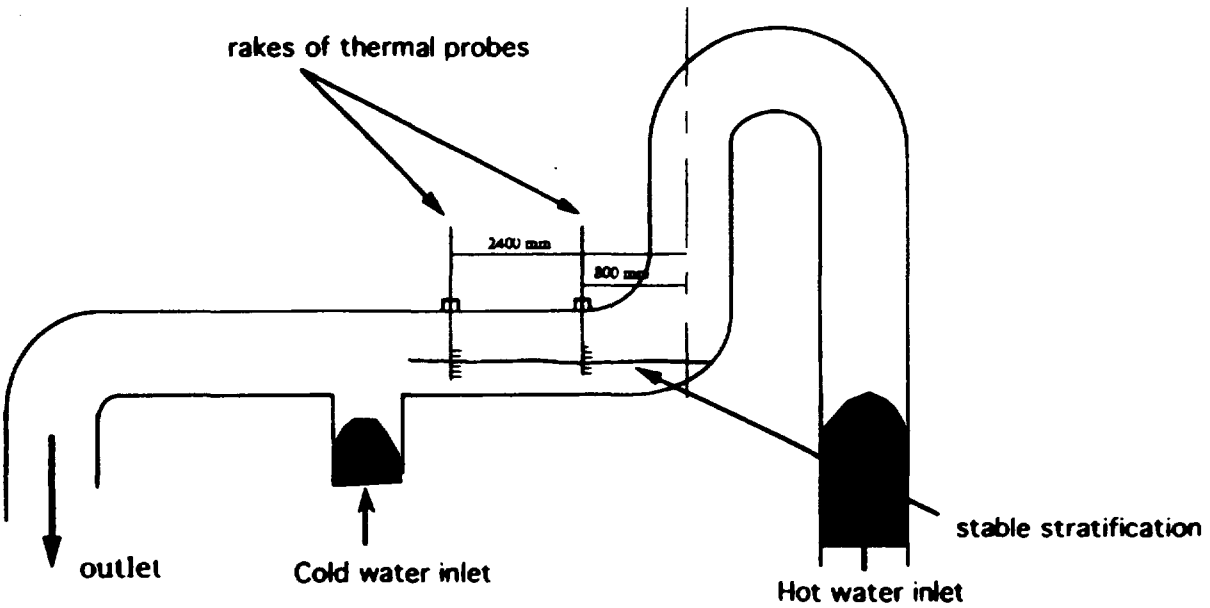

Figure 1 : Sketch of the Super Nimbus mock-up

This material is very sensitive to temperature, therefore the temperature variation has to be limited to the range [20°C to 50°C], which is very far from the temperature existing in the real situation.

Figure 2 presents briefly the model geometry. The diameter of pipes is 0.4m, the thickness of the perspex (material which unlike ferritic pipes, is a very poor thermal conductor) is 2.4cm. The cold and hot leg are supplied through a loop. It is possible to set flow rates from 1 l/s to 8 l/s and set a difference of temperature, between hot and cold leg, up to 30°C.

Only temperature measurements are recorded. Vertical temperature profiles within the pipe are measured with 2 rakes of thermal probes. The time record is then treated to provide mean temperature, temperature variance, and spectrum at the location considered.

Several tests have been conducted, (some of them up to 5 times) to ensure repeatability of the phenomena. These experimental data have been compared to numerical results obtained with a CFD code.

Fluo

A sketch of the experimental facility is presented on figure (2). Made of perspex it allows good visualisations (Laser techniques can also be used to investigate velocity fields). One side wall is made of conducting metal. The experimental facility has been built at CEA and all measurements have been performed by Tenchine and Baroill [6] at CEA.

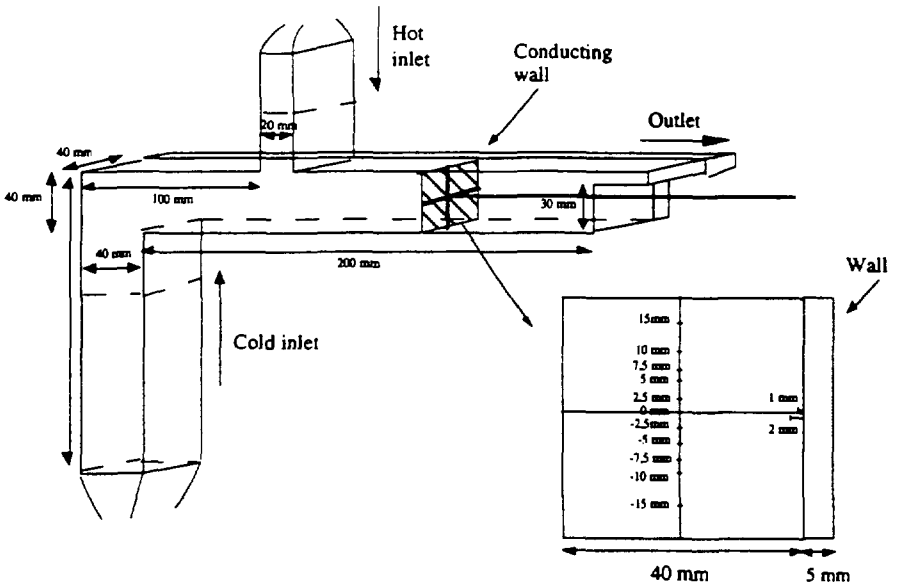

Figure 2 : Geometry of the mock-up FLUO

This small size mock-up (see dimensions in mm), is composed of two legs connected together with a T junction. A cold flow is injected upwards through the vertical pipe and forms an horizontal flow after the elbow. A hot flow is injected downwards through the upper vertical pipe. Flow rates and temperatures of cold and hot legs are monitored to stay as stable as possible. Regarding measurements, thermocouples have been used for temperature. Two rakes of thermocouples forming a cross (see sketch 4) allow to access temperature profiles. For each experiment, four locations along the x direction have been studied in detail :20 mm, 60 mm, 100mm and 160 mm after the T junction.

2. COMPUTATIONAL APPROACH OF THE THERMAL PROBLEM

Experimental approaches, although very informative, have some limitations. For example, no measurements are available on the velocity field in the present case. Moreover, small scale models are often unable to satisfy the similarity criteria required for adequate representation of real phenomena, or to respect real boundary conditions, leading numerical approaches to gain some interest.

Moreover, in the last decade, increasing computer capabilities (core memory and CPU cost) and the emergence of adequate Navier Stokes numerical solvers, allowed three-dimensional flow problems computation with accurate space discretization. ESTET, developed at the Laboratoire National d'Hydraulique, is a 3D finite volumes code able to handle a wide range of fluid mechanics applications. This code is developped under quality assurance policy, has been validated against numerous experiments, and has been used extensively in the past years.

This part of the paper reports briefly the equations solved as well as the numerical methods used before describing results obtained on the SUPER NIMBUS geometry.

2.1 Set of equations

Flows studied in the present paper are restricted to single phase flow satisfying the Reynolds averaged Navier Stokes equations. Let x_i $i = 1$ *to* 3 be a cartesian system of coordinates, then the system of averaged equations (mass, momentum, thermal energy conservation) required for the thermal hydraulic computations reads :

$$\frac{\partial \rho}{\partial t} + \frac{\partial \rho U_i}{\partial x_i} = 0 \tag{1}$$

$$\frac{\partial U_i}{\partial t} + U_j \frac{\partial U_i}{\partial x_j} = \frac{1}{\rho}\frac{\partial}{\partial x_j}\left(\mu_m\left(\frac{\partial U_i}{\partial x_j} + \frac{\partial U_j}{\partial x_i}\right) - \rho\,\overline{u_i u_j}\right) - \frac{1}{\rho}\frac{\partial p^*}{\partial x_i} - \frac{\rho - \rho_o}{\rho} g_i \tag{2}$$

$$\frac{\partial T}{\partial t} + U_i \frac{\partial T}{\partial x_i} = \frac{1}{\rho C_p}\frac{\partial}{\partial x_i}\left(K_m - \rho C_p\,\overline{u_i T}\right) \tag{3}$$

In these equations, U_i are the components of the mean velocity, u_i the velocity fluctuation, p^* is the pressure difference from an hydrostatic equilibrium involving a reference density ρ_o, T is the mean temperature, μ_m and K_m are the molecular viscosity and conductivity. The eddy viscosity concept has been used to close the sytem. It means that Reynolds stress tensor and turbulent heat flux are assumed to be colinear to mean strain tensor and mean temperature gradient. Spectral equilibrium as well as constant energy transfer (of value ε) along the inertial subrange is assumed, leading to the following expressions.

$$-\rho\,\overline{u_i u_j} = \mu_t\left(\frac{\partial U_i}{\partial x_j} + \frac{\partial U_j}{\partial x_i}\right) - \frac{2}{3}\left(\rho k \delta_{ij} + \mu_t \frac{\partial U_l}{\partial x_l}\right) \tag{4}$$

$$-\rho C_p\,\overline{u_i T} = K_t \frac{\partial T}{\partial x_i} \tag{5}$$

with

$$\mu_t = \rho C_\mu \frac{k^2}{\varepsilon} \tag{6}$$

$$K_t = \frac{\rho C_\mu}{\sigma_T}\frac{k^2}{\varepsilon} \tag{7}$$

The determination of k and ε the turbulent kinetic energy and its dissipation rate respectively, is done by the following transport equations (see Launder [7]).

$$\begin{cases} \dfrac{\partial k}{\partial t} + \vec{U}\ grad\ k = \dfrac{1}{\rho}\,div\left((\mu + \dfrac{\mu_t}{\sigma_k})grad\ k\right) + P + G - \varepsilon & (6) \\[2ex] \dfrac{\partial \varepsilon}{\partial t} + \vec{U}\ grad\ \varepsilon = \dfrac{1}{\rho}\,div\left((\mu + \dfrac{\mu_t}{\sigma_\varepsilon})grad\ \varepsilon\right) + C_{\varepsilon_1}\dfrac{\varepsilon}{k}(P + (1 - C_{\varepsilon_3})G) - C_{\varepsilon_2}\dfrac{\varepsilon^2}{k} & (7) \end{cases}$$

where :

$$P = \left(\frac{\mu_t}{\rho}\left(\frac{\partial U_i}{\partial x_j} + \frac{\partial U_j}{\partial x_i}\right) - \frac{2}{3}\left(k + \frac{\mu_t}{\rho}\frac{\partial U_l}{\partial x_l}\delta_{ij}\right)\right)\frac{\partial u_i}{\partial x_j} \tag{8}$$

and

$$G = \frac{K_t}{\rho}\beta g_i \frac{\partial T}{\partial x_i} \tag{9}$$

The choice of the constant $C_{\epsilon 3}$ is still under discussion. For the present calculation, we follow Viollet [8].

$$\begin{cases} C_{\epsilon 3} = 1 & \text{if } G \leq 0 \text{ stable stratified flow} \\ C_{\epsilon 3} = 0 & \text{if } G \geq 0 \text{ unstable stratified flow} \end{cases} \tag{10}$$

This term, relating buoyancy effects and turbulence, is of importance in stratified flows, since it ensures the stability of such stratified flows by inhibiting the turbulent mixing at the interface.

An equation for the temperature fluctuations variance has been used. It relies on a simplified modelling for the dissipation term (see Rodi [9]), assuming a constant ratio R between dynamical and thermal turbulent length scales.

$$\begin{aligned} \frac{\partial \theta^2}{\partial t} + u_i \frac{\partial \theta^2}{\partial x_i} = & \frac{\partial}{\partial x_i}\left(\left(K_m + \frac{C_\mu}{\sigma_\theta}\frac{k^2}{\varepsilon}\right)\frac{\partial \theta^2}{\partial x_i}\right) \\ & + 2\frac{C_\mu}{\sigma_T}\frac{k^2}{\varepsilon}\left(\frac{\partial T}{\partial x_i}\right)^2 - \frac{1}{R}\frac{\varepsilon}{k}\theta^2 \end{aligned} \tag{11}$$

2.2 Numerical methods

ESTET uses a finite differences - finite volumes method based upon a fractional step technique (see Chorin [10]), discretizing the continuous problem into a time series. Within each time step $[t^n, t^{n+1}]$, intermediate values corresponding to the convective, diffusive, and continuity operators, are introduced.

Advection for all variables

This step is solved by a three dimensional characteristic method. It has limited numerical diffusion due to the use of a third order interpolation.

Diffusion and source terms for mean variables

The treatment of diffusion uses a spatial splitting technique, transforming the 3D diffusion operator into 1D problems. Then the resulting three diagonal systems (one for each coordinate direction) are easily handled by a Gauss elimination method.

Continuity equation

A Poisson equation is derived by combining continuity and momentum equation. It is solved by a conjugate residual method.

k and ε diffusion and source terms

For the evolution of k and ε, a partially implicit treatment using increments of k and ε has been implemented. It splits k and ε along the coordinate directions while keeping the two variables coupled. Viscosity in the diffusion term and mean variable gradient appearing in some source terms are however treated explicitly.

2.3 Boundary conditions

At each inlet velocity and turbulent quantities are imposed. In order to set the best possible inlet conditions, a flow calculation of the inverse U shaped elbow upstream of the present geometry has been performed. The outlet of this first calculation is used as inlet for the present calculation.

At the wall, a wall function approach is used. It supposes the existence of a logarithmic sublayer within which the first fluid node is advised to be located. The main hypothesis is to suppose that the flow and the eddy viscosity may be approached by the following laws.

$$\nu_t = \kappa u_* y \quad with \quad \frac{U}{u_*} = \frac{1}{\kappa} log\left(\frac{u_* y}{\nu}\right) + C \tag{12}$$

$$k = \frac{u_*^2}{\sqrt{C_\mu}} \quad \varepsilon = \frac{u_*^3}{\kappa\, y} \tag{13}$$

then boundary conditions on velocity are

$$\vec{u}\,\vec{n} = 0 \quad and \quad \frac{\partial}{\partial n}\left(\vec{U}\,\vec{\tau}\right) = \frac{u_*}{\kappa y_n} \quad or \quad \frac{u_*^2}{\nu_t} \tag{14}$$

Walls being considered adiabatic in the present calculation, a zero flux option is used for the mean temperature and the temperature fluctuation variance.

The pressure condition used is $\frac{\partial p^*}{\partial n} = 0$ on the boundary. At the exit the condition applied is $\frac{\partial}{\partial n}\left(\frac{\partial p^*}{\partial \tau}\right) = 0$ meaning that the pressure profile is conserved in the last two sections.

The time step is chosen to satisfy numerical stability criteria like the local Courant and Fourier numbers.

2.4 Grid generation

The computer program ESTET solves the equation mentioned above on an orthogonal grid with slanted boundary cells which allow a good description of complex 3D geometries. However, because of the difficulty of describing complex geometries with purely orthogonal grid, an orthogonal curvilinear version of the ESTET code has been implemented. For piping systems, only one curvilinear direction is required. In practice, a section is meshed with a 2D cartesian grid, and is then duplicated along a curvilinear path to create the final mesh, when necessary.

3. CALCULATION RESULTS FOR SUPER NIMBUS

In the present case, 4 sets of conditions have been investigated. In each case the flow rate of the cold and hot leg is 4 liter/s but the temperature difference between the two legs is varying between 5 $°C$ and 30$°C$, which leads to Froude numbers varying from 0.45 to 0.16

The computation starts with the pipe initially filled with hot water Once the isothermal flow has reached a converged state, a cold flow is injected through the vertical pipe. Gravity effects tend to prevent the cold jet from penetrating the hot flow and force it to spread out laterally. A cold counterflow is created at the bottom portion of the pipe section, and flows towards the elbow, several meters away

Once this cold layer has reached the elbow, kinetic energy is transformed in potential energy and a wave goes backwards and increases the thickness of the cold section. Due to the reduced section, (more than halved), the hot flow accelerates and creates velocity gradients at the interface. However, no increase in turbulent diffusivity is predicted numerically, (due to the turbulence inhibiting terms in the dissipation equation), which explains that sharp temperature gradients can be predicted.

Once the converged states are obtained, experimental results can be compared with numerical ones, at the two sections where experimental profiles have been recorded. Figure 3 presents the corresponding profiles. Dots and crosses represent the experimental data and the lines represent the calculated results. These curves show the influence of the Froude number on the stratification phenomena, and tend to prove that the numerical approach can be of interest to study phenomena as complex as stratified flow. The experimental behaviour is well reproduced numerically, even if a close examination shows that the temperature gradient through the interface is slightly underestimated.

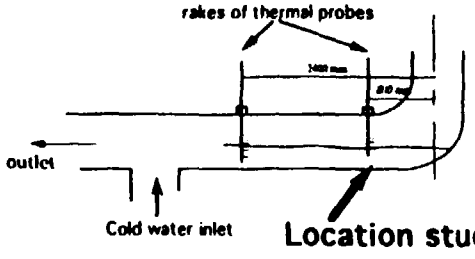

Cas	ΔT	Rho hot	Rho cold	Froude number
cas11	5	998,25	997,50	0,45
cas12	10	994,70	997,86	0,20
cas13	20	992,80	998,70	0,21
cas14	30	987,50	987,50	0,16

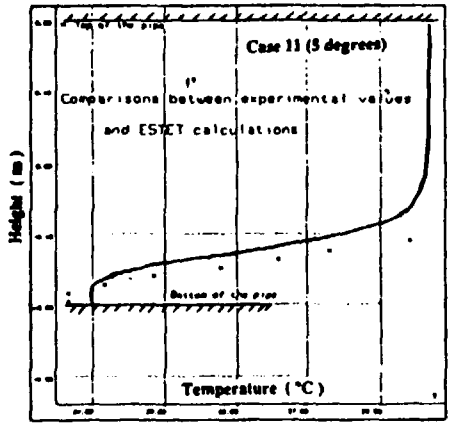

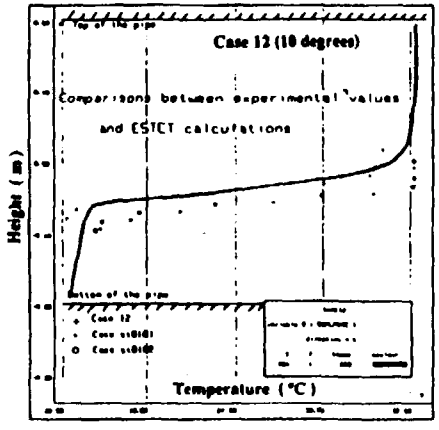

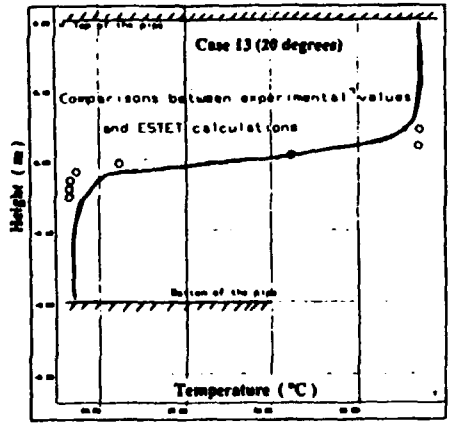

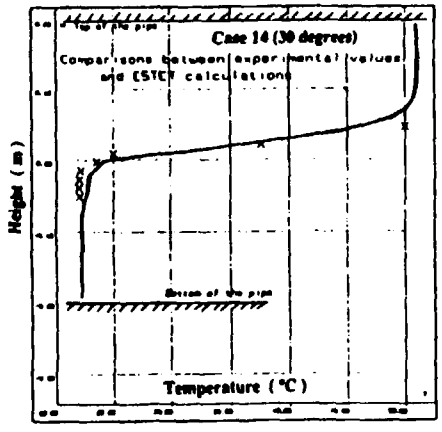

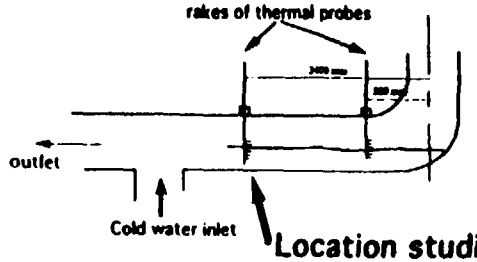

Cas	ΔT	Rho hot	Rho cold	Froude number
cas11	5	998,25	997,50	0,45
cas12	10	994,70	997,86	0,20
cas13	20	992,80	998,70	0,21
cas14	30	987,50	987,50	0,16

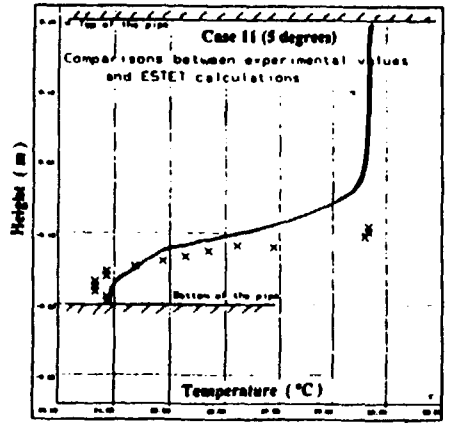

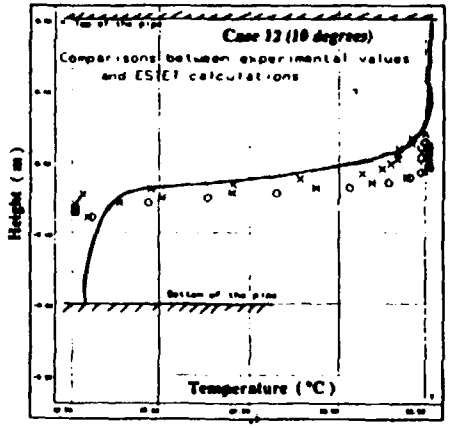

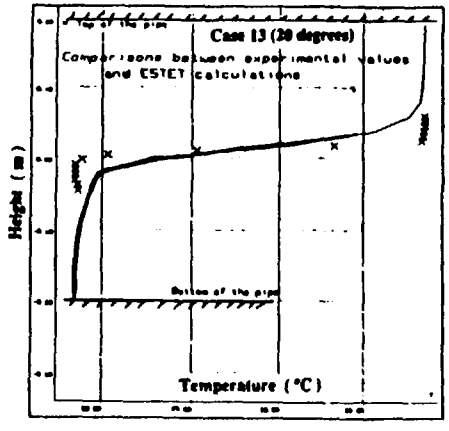

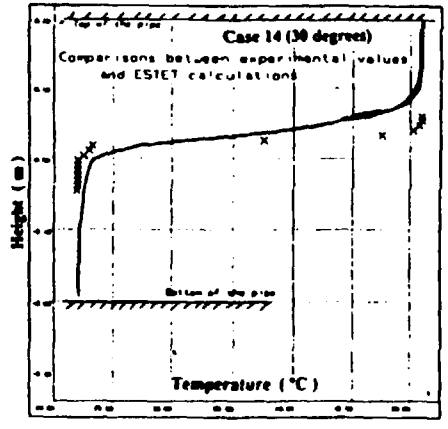

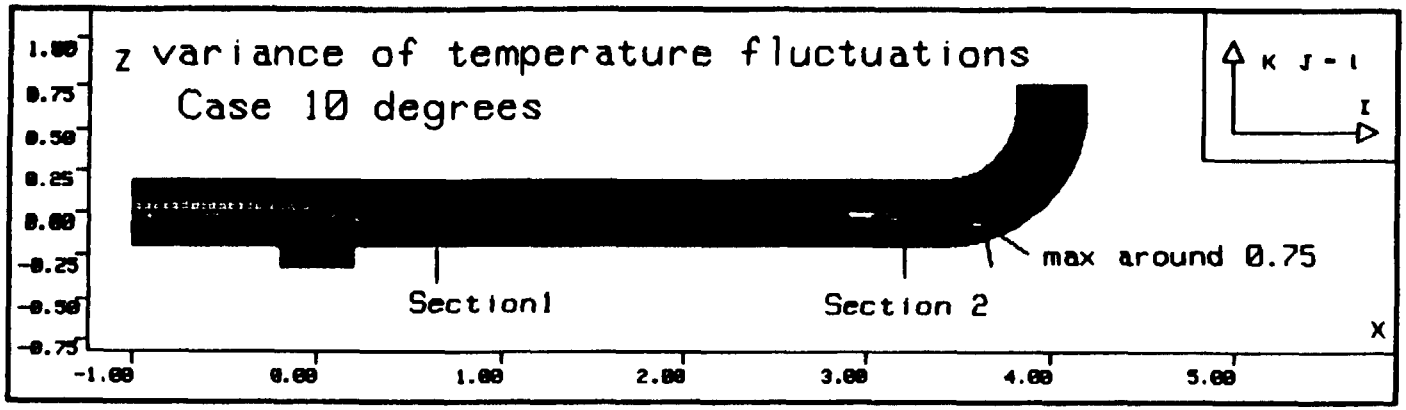

Temperature fluctuations (section 1)

Comparisons between calculated and experimental data

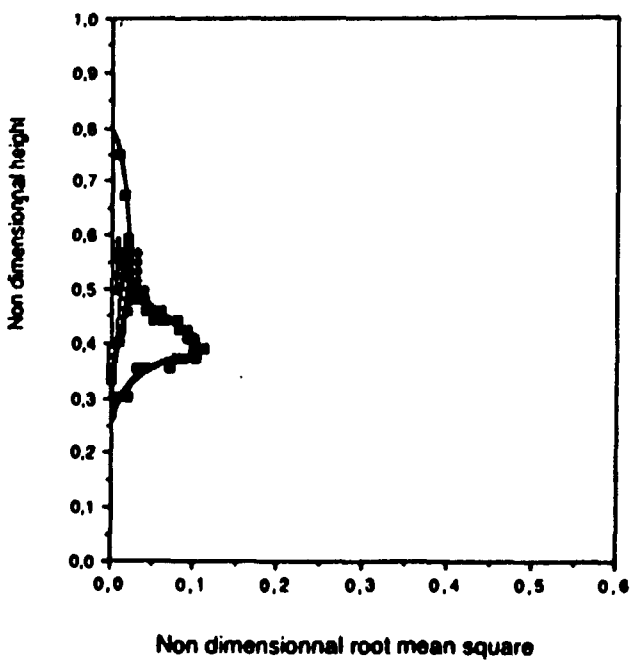

Temperature fluctuations (section 2)

Comparisons between experimental and calculated data

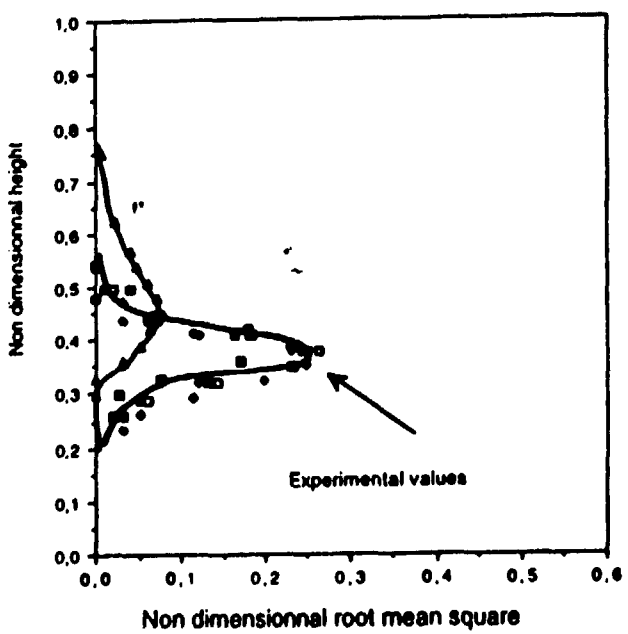

The higher Froude number (corresponding here to a temperature difference of $5°C$ between the two legs) is barely able to create a stratification up to the elbow. The thickness of the counterflow is small experimentally and numerically. Moreover, both experimentally and numerically, it takes a very long time (about 2000s of simulation) for a converged state to be reached. On the contrary, the lower Froude number, (corresponding here to a 30° difference) reaches a stable state quickly (a simulation time of less than 500s is required). This is due to the fact that gravity effects are much stronger, and that it is much easier for the heavier cold flow to proceed against the incoming hot flow.

Some measurements and numerical comparisons have been done regarding the temperature fluctuation phenomena. Unlike in the experiment, only statistical values (time averaged) are accessible numerically, which prevent for exemple the possibility of obtaining spectral information. In the present case, the root mean square of the temperature fluctuation has been studied. As is shown in figure 5 , it seems that the present modelling, (or approach) fails to reproduce correctly the phenomena. The calculations underpredict dramatically the variance recorded experimentally. A detailed study of the temperature signal recorded on the experimental facility (see the spectrum of the temperature signal presented in figure 6) shows that the energy contained in the signal is mostly due to large coherent structures (of Kelvin Helmoltz type) which are superimposed on classical turbulent phenomena. Therefore it is quite normal that a k-ε approach fails to reproduce accurately the fluctuating phenomena. A large eddy-simulation would certainely be a much more appropriate way to tackle the fluctuating phenomena created within the stratification, near the elbow.

In a real case, the wall is made of steel which is a good thermal conductor. Therefore heat transfer through the wall should be accounted for.

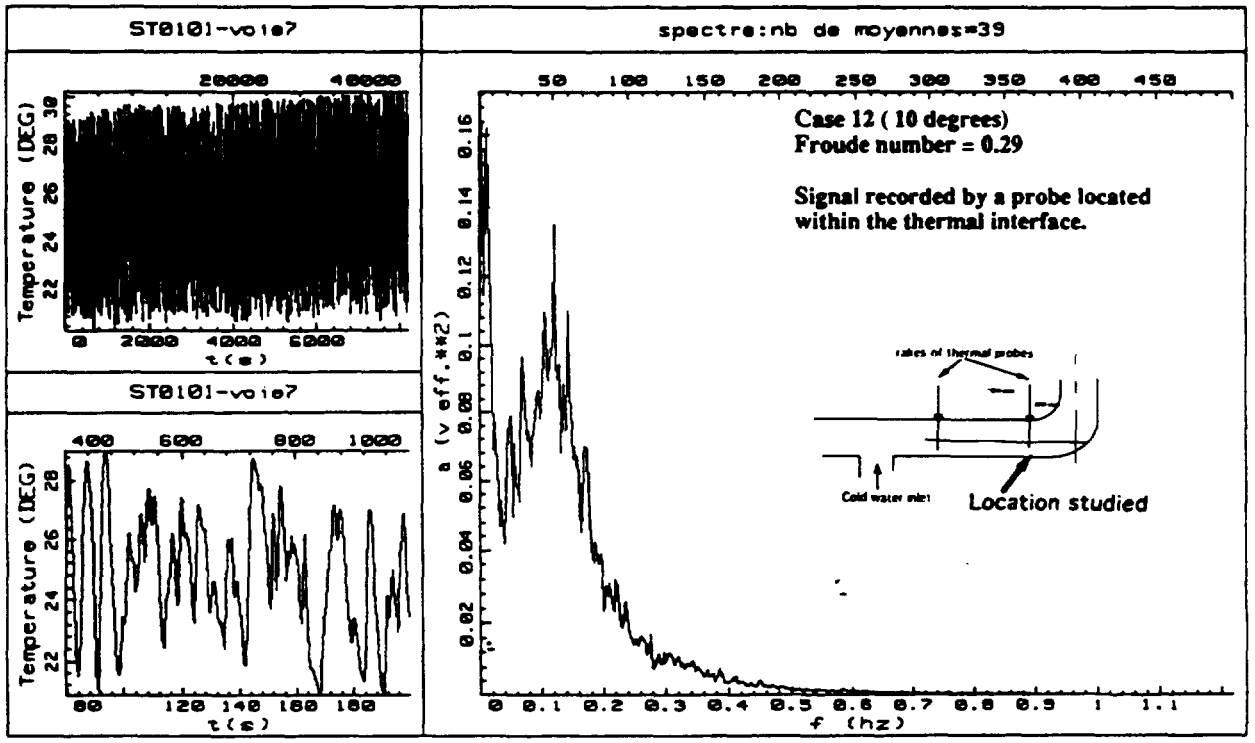

Figure 6 : Time signal and Spectrum

4. TAKING THE THERMAL COUPLING BETWEEN FLUID AND SOLID INTO ACCOUNT

In many industrial applications, a thermal coupling exists between a fluid and the solid body by which it is surrounded. Among topics of interest, studied at EDF, thermal shocks arising in piping systems of nuclear plants can be pointed out. These shocks originate from a quick variation of the flow temperature. This may lead to mechanical damages (like cracks). Of course, other fields, like heat exchangers, electrical devices, etc... have to address the same kind of problem.

Experimental approaches have been used extensively in the past, but they may become very costly (when dealing with a very hot fluid under high pressure for example). Moreover, they often lack the flexibility needed when a parametric study is desired. On the other hand, with powerful computer facilities now available at affordable cost, numerical approaches become more and more promising to accurately predict thermal phenomena and their effects.

In order to extend the capabilities of CFD codes, several options have been examined, like the extension of the grid to mesh both solid and fluid domains with a common grid. Due to optimisation motivations (in memory and cpu costs) a more promising procedure has been followed. The two domains have been geometrically and numerically decoupled, and the solid part treated by a finite element approach (code SYRTHES [11] [12]). This allows a fine description of the solid geometry (which is often complex). Once the thermal field obtained, the non structured mesh and the temperature at each node can be used almost directly by a general purpose mechanical code. Thus mechanical consequences of a thermal loading caused by a temperature step in the flow can be achieved with reasonable effort, and time.

5. CALCULATION RESULTS FOR FLUO

Four cases have been simulated numerically. The following table is presenting the operating conditions corresponding to these cases.

	Case 1	Case 2	Case 3	Case 4
V_{cold}	0.026	0.026	0.026	0.052
T_{cold}	20	20	15	15
V_{hot}	0.026	0.026	0.026	0.052
T_{hot}	40	30	55	55

Figure 7 : Test matrix (velocity in m/s and temperature in degree C)

The two independent grids used (one structured grid for the fluid, and one unstructured grid for the solid) are presented on figure 8.

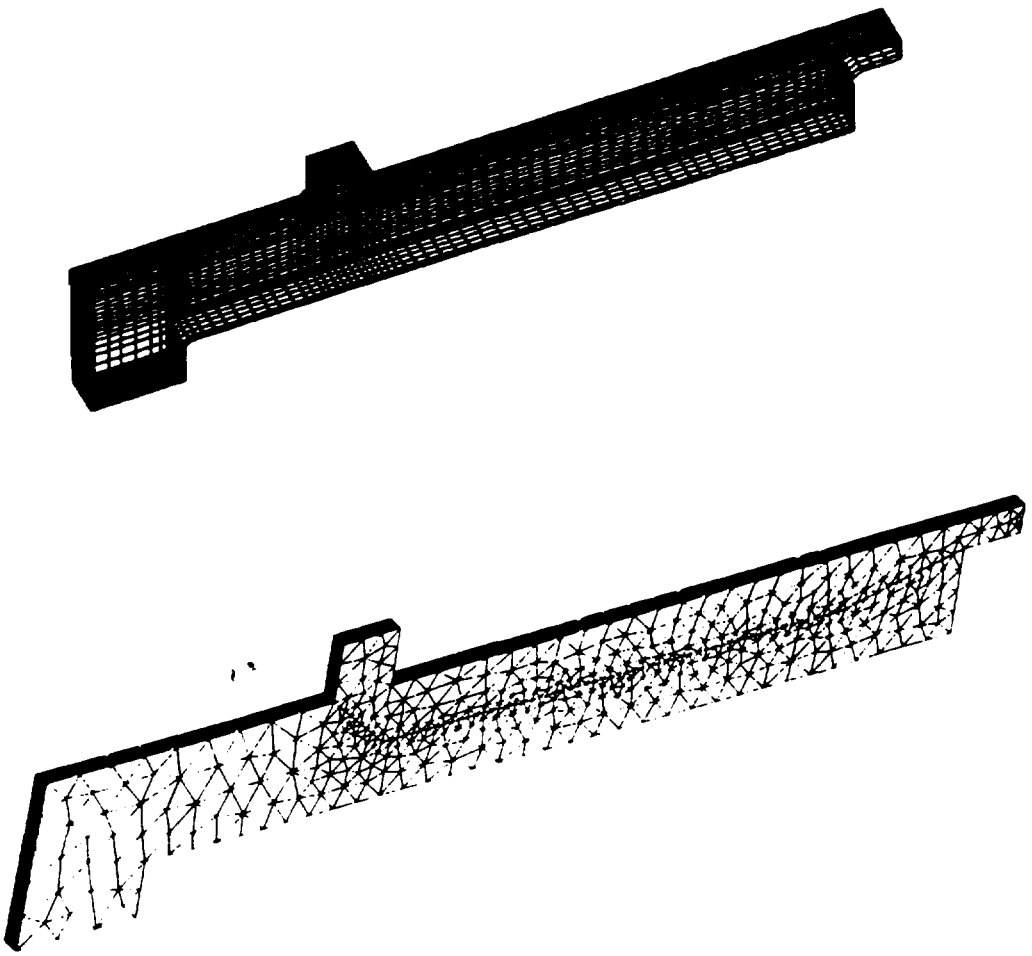

Figure 8 : Grids used for the calculation

Initially the simulation starts with a field set at a uniformally cold temperature, then at time $t = 0$, a hot flow is injected through the upper vertical pipe. Due to gravity effect a co-courant stratification forms downstream. It is interesting to underline the fact that ESTET is able to predict (like in the experiment) that not counter-flow forms in this particular geometry, although the Froude number is small enough to allow the creation of such a counter-flow in different geometries as has been demonstrated for the Super Nimbus case. After some time, a converged state is reached. Figure 9 presents respectively the velocity field, the temperature field and the temperature fluctuation variance on the middle plane for case 4. The hot jet is influencing the incoming cold flow, however for the present case it can be seen that the mixing between the two layers stays quite small. This is partly due to the fact that at the interface the stably stratified flow tend to inhibit the turbulent diffusion between the two layers. At the junction, there is simultaneously high temperature gradients and turbulence. Therefore production of temperature fluctuations exists. Then due to the stable stratification effect, a decrease in the level of temperature variance is predicted. The same type of figures could be presented for all cases.

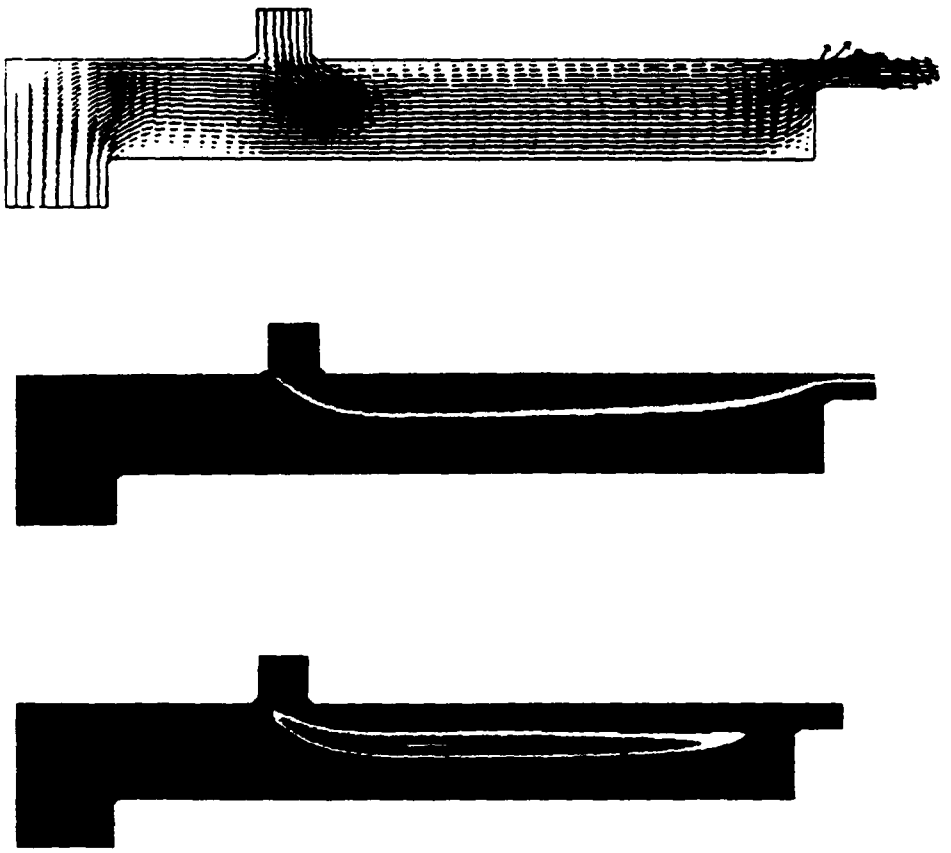

Figure 9 : Velocity and temperature, and rms temperature fluctuations fields on the middle plane

The simulation presented here includes the calculation of the thermal field within the solid wall. At the beginning, wall thermal inertia is leading to observe temperature differences between the two sides of the solid wall. However after some time the following isothermals are obtained within the wall.

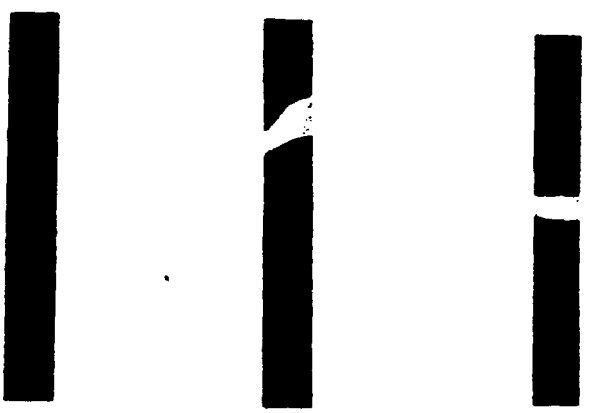

Figure 10 : Solid temperature in section 100mm,10s, 20s and 100s after injection

The same phenomena is illustrated by figure 11, where it is clear that conduction through the wall takes place and leads to heat the cold fluid layer in contact with the solid wall.

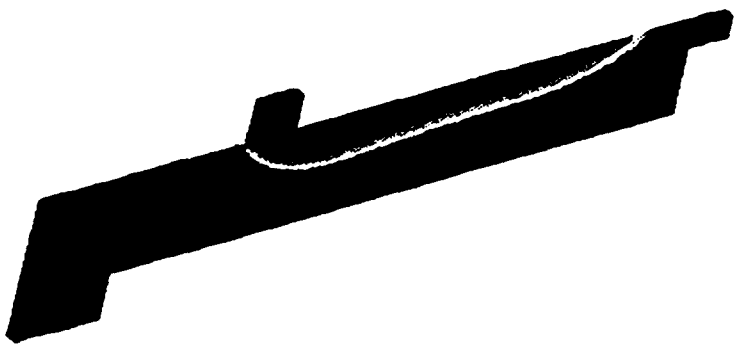

Figure 11 : Solid temperature

Some more quantitative comparisons have been done between experimental data and numerical results. Picture 12 presents non dimensional comparisons of temperature profiles and temperature fluctuations profiles at sections 20mm, 60mm, 100mm and 160mm for case 4.

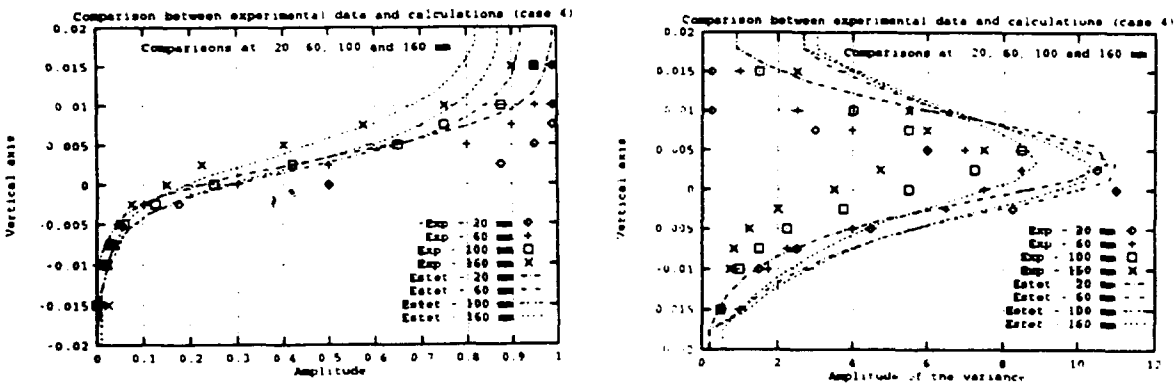

Figure 12 : Temperature and rms fluctuations profiles for case 4

5. INDUSTRIAL APPLICATIONS INCLUDING A THERMAL COUPLING BETWEEN FLUID AND SOLID

The goal of this small chapter is just to present briefly an industrial case which has been studied with the numerical tool presented in this paper. It consists in a T junction where a cold flow and a warm one meet. A stratified flow is created and induces a complex thermal distribution inside the wall. Meshes used for the flow calculation and the solid calculation are presented. The thermal distribution is presented as well. More complex cases will be presented during the talk.

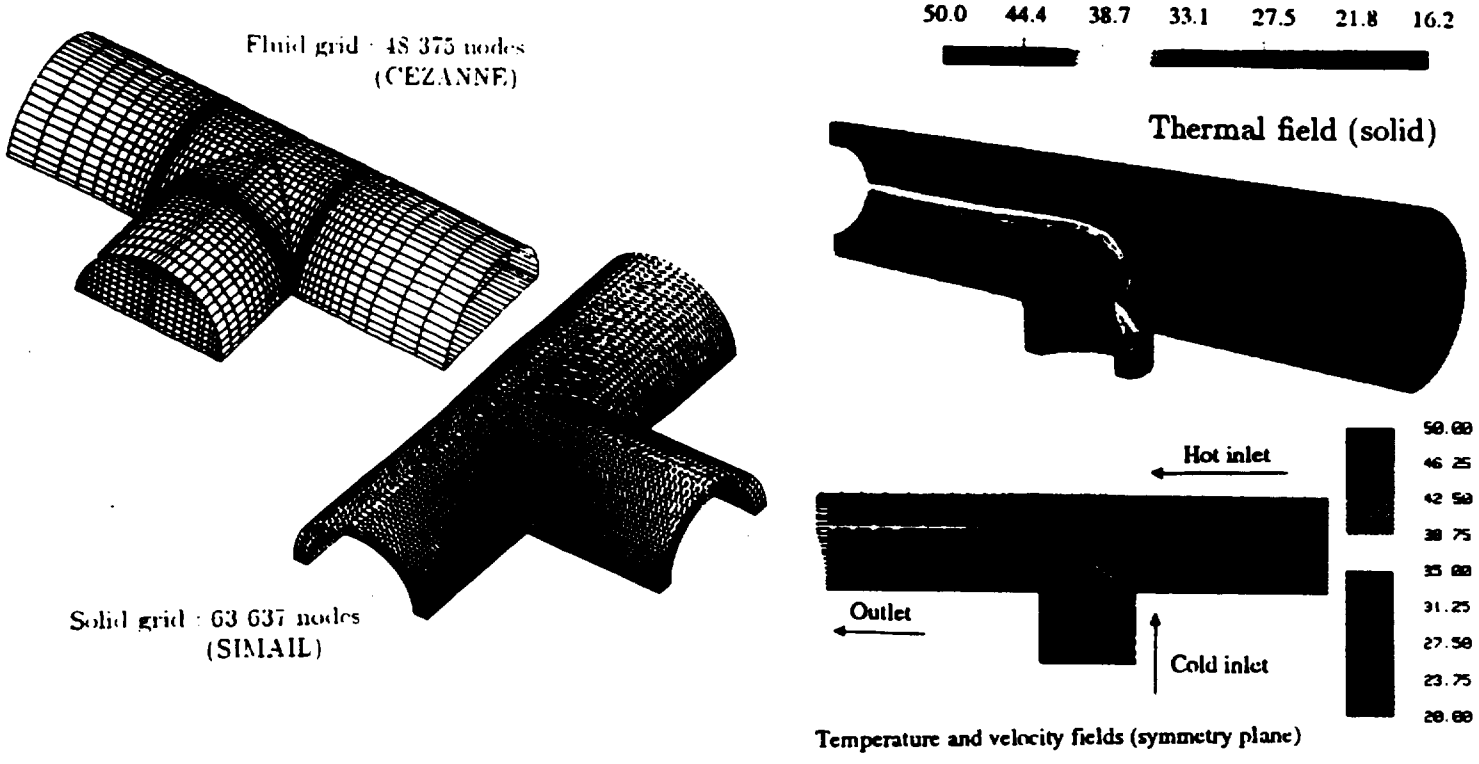

Figure 13 : Thermal stratification at a T junction

6. CONCLUSIONS

According to the Froude number, stratified flows may appear. This has been verified on several experimental models. Moreover it has also been demonstrated that numerical tools are able to simulate stratified flows in complex three-dimensional geometries.

Fair agreement between experimental results and numerical calculations is observed for mean quantities. This gives some confidence in begining to use numerical tools to gain some understanding in phenomena as complex as stratified flow.

On the contrary it seems that the present modelling of the temperature fluctuation variance fails to reproduce accurately the fluctuating phenomena observed experimentally.

ACKNOWLEDGEMENT

Experimental results (Super Nimbus) presented in this paper are part of a "tripartite" agreement between CEA, EDF and Framatome. Fluo is part of "bipartite" agreement between CEA and EDF.

REFERENCES

[1] PENIGUEL C., STEPHAN J.M.
"Thermalhydraulic study of a stratified flow in a piping elbow
(Application to the model COUFAST) NURETH-5, September 1992 Salt Lake City."

[2] STEPHAN J.M., CARON J., RIOLAND M.
"COUFAST : Experimental study of mechanical consequences
of thermal stratification on a piping elbow", ASME-PVP june 1992 New Orleans.

[3] PENIGUEL C., HECKER M.
"Thermal hydraulic study of a stratified flow in an elbow geometry"
model Super Nimus. NURETH-6, Grenoble october 1993

[4] PENIGUEL C.
"Numerical study of a thermally stratified flow and
its interaction with a conducting wall. 4th ISSF July 1994

[5] PREUD'HOMME E.
" Non invasive techniques development for local
thermal hydraulic analysis of dead leags and stratified pipes in PWR's"
JSME - ASME Joint Int Conf on Nuclear Engineering. November 1991 Tokyo

[6] TENCHINE D., BARROIL J
"Fluctuations de temperature en ecoulement stratifies
Attenuation des fluctuations de temperature. STR/LES/92-05"

[7] LAUNDER B.E., SPALDING D.B.
"The numerical computation of turbulent flows,Comp. Meth Applied Mech. Eng 3 (1974).

[8] VIOLLET P.L.
"The modelling of turbulent recirculating flows for the purpose of reactor
thermal-hydraulic analysis" Nuclear Engineering Des 99, 365-377 (1987).

[9] RODI W.
"Turbulence Models and their Application in Hydraulics",
IARH, Delft, The Netherlands (1980).

[10] CHORIN A.J.
"Numerical Solution of incompressible flow problem", SIAM J. Numer. Anal. 2 (1968).

[11] PENIGUEL C., RUPP I.
"A numerical method for thermally coupled Fluid solid problems
Num Meth in thermal problems. Swansea July 1993

[12] PENIGUEL C., RUPP I.
A Numerical Approach for Thermally Coupled Fluid and Solid Problems in Complex
Geometries *3rd Int conf Heat Transfer* U.K., August 1994, Southampton